

# A newly identified G-quadruplex as a potential target regulating Bcl-2 expression

Hongxia Sun<sup>a,\*</sup>, Junfeng Xiang<sup>a</sup>, Yunhua Shi<sup>a,b</sup>, Qianfan Yang<sup>a</sup>, Aijiao Guan<sup>a</sup>, Qian Li<sup>a</sup>, Lijia Yu<sup>a,b</sup>, Qian Shang<sup>a</sup>, Hong Zhang<sup>a</sup>, Yalin Tang<sup>a,\*\*</sup>, Guangzhi Xu<sup>a</sup>

<sup>a</sup> Beijing National Laboratory for Molecular Sciences, State Key Laboratory for Structural Chemistry of Unstable and Stable Species, Institute of Chemistry, Chinese Academy of Sciences, Beijing 100190, PR China

<sup>b</sup> University of Chinese Academy of Sciences, Yuquan Road 19(A), Shijingshan District, Beijing 100049, PR China

## ARTICLE INFO

### Article history:

Received 21 April 2014

Received in revised form 10 July 2014

Accepted 21 July 2014

Available online 30 July 2014

### Keywords:

Bcl-2 P1 promoter

G-quadruplex

Anticancer therapeutic target

Phenanthroline-dicarboxylate

Spectroscopy

Dual-luciferase reporter assay

## ABSTRACT

**Background:** A new G-quadruplex structure located in the B-cell CLL/lymphoma 2 (Bcl-2) P1 promoter and its physiological function related to Bcl-2 transcription have been studied to find a potential anticancer therapeutic target. **Methods:** Absorption, polyacrylamide gel electrophoresis, fluorescence, circular dichroism, and nuclear magnetic resonance spectra have been employed to determine G-quadruplex structure and the interaction between G-quadruplex and phenanthroline-dicarboxylate. Real time polymerase chain reaction and luciferase assay were done to assess the physiological function of the G-quadruplex structure.

**Results:** The UV-melting and polyacrylamide gel electrophoresis studies show that the p32 DNA sequence forms an intramolecular G-quadruplex structure. Circular dichroism and nuclear magnetic resonance spectra indicate that the G-quadruplex is a hybrid-type structure with four G-tetrads. Fluorescence spectra show that a phenanthroline derivative has a higher binding affinity for p32 G-quadruplex than duplex. Further circular dichroism and nuclear magnetic resonance studies indicate that the phenanthroline derivative can regulate p32 G-quadruplex conformation. Real time polymerase chain reaction and luciferase assays show that the phenanthroline derivative has down-modulated Bcl-2 transcription activity in a concentration-dependent manner. However, no such effect was observed when p32 G-quadruplex was denatured through base mutation.

**Conclusion:** The newly identified G-quadruplex located in the P1 promoter of Bcl-2 oncogene is intimately related with Bcl-2 transcription activity, which may be a promising anticancer therapeutic target.

**General significance:** The newly identified G-quadruplex in the Bcl-2 P1 promoter may be a novel anticancer therapeutic target.

© 2014 Elsevier B.V. All rights reserved.

## 1. Introduction

The Bcl-2 (B-cell CLL/lymphoma 2) gene is a mitochondrial membrane protein involved in the control of programmed cell death, functioned as an apoptosis inhibitor [1,2]. The overexpression of Bcl-2 gene occurs in a wide range of human cancers [3,4], which reduces the rate of cell death and also interferes with the therapeutic action by resisting chemotherapy-induced apoptosis [5,6]. Due to the crucial role in preserving a balance between cell death and survival, Bcl-2 gene has been considered as an important target for developing anti-

cancer compounds. The transcription of the Bcl-2 gene is controlled by two promoters, P1 and P2 [7]. The P2 promoter contains two transcription-inhibitory elements and an open reading frame, which behaves as a posttranscriptional down-regulator [8]. The P1 promoter, from which 90 to 95% of transcripts initiate [9], appears to be the primary driving force that regulates Bcl-2 transcription. Many transcription factors, including SP1, WT1, E2F, NGF, and IGF, bind to this region, indicating the importance for P1 promoter regulation [10].

The P1 promoter, especially the region upstream of the translation initiation site, is highly GC-rich [11], and the sequence within this region may tend to form G-quadruplex, a special secondary structure mediated by Hoogsteen hydrogen bonding [12,13]. Two regions located at –19 bp and –176 bp upstream of the P1 promoter have been validated to form G-quadruplexes [10,14–17]. Recently, we find another sequence (labeled as p32; Fig. 1a) located in the Bcl-2 regulatory region –451 bp upstream of P1 promoter also exhibits G-quadruplex-forming tendency. There is research indicating deletion of the region in which p32 located causes a reduction in Bcl-2 gene transcription [18], implying the importance of this region in transcription activity. It is possible the p32

**Abbreviations:** Bcl-2, (B-cell CLL/lymphoma 2); (PD), phenanthroline-dicarboxylate; (PAGE), polyacrylamide gel electrophoresis; (NMR), nuclear magnetic resonance; (CD), circular dichroism; (PCR), polymerase chain reaction; (ILPR), insulin-linked polymorphic region; (IGF-1), insulin-like growth factor-1

\* Correspondence to: H. Sun, Institute of Chemistry, Chinese Academy of Sciences, Beijing 100190, PR China. Tel.: +86 10 82617304; fax: +86 10 82617302.

\*\* Correspondence to: Y. Tang, Institute of Chemistry, Chinese Academy of Sciences, Beijing 100190, PR China. Tel./fax: +86 10 62522090.

E-mail addresses: [hongxsun@iccas.ac.cn](mailto:hongxsun@iccas.ac.cn) (H. Sun), [tangyl@iccas.ac.cn](mailto:tangyl@iccas.ac.cn) (Y. Tang).

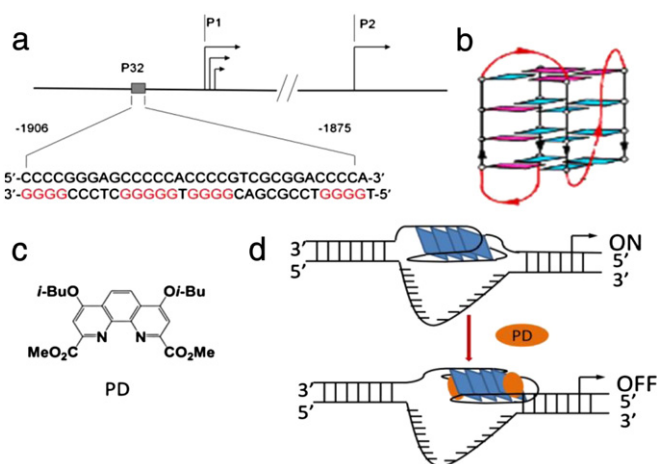


**Fig. 1.** The structures of the P1 promoter, p32 G-quadruplex, and PD. (a) Promoter structure of the human Bcl-2 gene. Shown in inset is the 32-mer sequence of the purine-rich strand upstream of the P1 promoter. (b) The schematic drawing of the folding topology of the p32 G-quadruplex. (c) Structural formula of phenanthroline-dicarboxylate (PD). (d) The scheme of the G-quadruplex related to the Bcl-2 gene expression and the down-modulation of Bcl-2 expression resulted from the G-quadruplex conformational transition induced by PD.

G-quadruplex in Bcl-2 P1 promoter is involved in Bcl-2 transcription activity just as the G-quadruplexes in c-myc, c-kit, and k-RAS oncogenes are [19]. It is known that G-quadruplexes have special physicochemical properties which make them druggable with a high degree of selectivity. To determine the p32 G-quadruplex and its function will be importantly significant for developing a therapeutic target in oncology.

Towards this goal, the p32 G-quadruplex structure and its physiological function have been studied. Based on the spectroscopic data, the G-quadruplex is identified to an intramolecular hybrid-type G-quadruplex structure composed of four G-tetrads (Fig. 1b), which has a high thermal stability under the physiological condition of  $K^+$ . The *in vitro* assays indicate that inhibiting the p32 G-quadruplex formation through base mutations or interacting with phenanthroline-dicarboxylate (PD, Fig. 1c), a novel phenanthroline derivative [20], causes an apparent reduction of Bcl-2 expression (Fig. 1d). These results present a compelling evidence of the G-quadruplex being intimately related with Bcl-2 transcription activity and also implicate the potential development of the p32 G-quadruplex as a novel therapeutic target. Furthermore, the reduced Bcl-2 expression by PD also provides a new therapeutic strategy besides stabilizing G-quadruplex by ligands.

## 2. Materials and methods

### 2.1. Sample preparation

The oligonucleotides including p32 (5'-TG<sub>4</sub>TCCGCGACG<sub>4</sub>TG<sub>5</sub>CTCCG<sub>4</sub>-3'), p32-mut (5'-TG<sub>4</sub>TGTCGCGACGTGGTGGTGGTCCCGGTG-3'), p32-com (5'-C<sub>4</sub>G<sub>3</sub>AGC<sub>5</sub>AC<sub>4</sub>GTCGCGAC<sub>4</sub>A-3') and d26 (5'-CAATCGGATCGAATTCGATCCGATTG-3') were purchased from Invitrogen (Beijing, China), purified by PAGE. Tris(hydroxymethyl)aminoethane (Tris) was purchased from Sigma. Analytical grade KCl was purchased from Beijing Chem. Co. Ultrapure water prepared by Milli-Q Gradient ultrapure water system (Millipore) was used throughout the experiments. The stock solutions of the oligonucleotides were prepared by dissolving oligonucleotides directly into 10 mM Tris-HCl buffer (pH 7.2).

### 2.2. Spectroscopy measurement

Ultraviolet (UV) spectra were measured on an Agilent 8453 spectrophotometer at the wavelength range 190–1100 nm using a 1 cm path cell. The absorbance was monitored at 295 nm while the temperature was increased from 25 to 95 °C at a rate of 2.0 °C min<sup>-1</sup>. The thermal

denaturing temperature values were determined using the van't Hoff method.

The polyacrylamide gel electrophoresis (PAGE) was conducted in 1× TBE (Tris base-boric acid-EDTA) buffer solution containing 100 mM KCl with 15% native gels. The gels were run at 100 V for 1 h at room temperature. Then the gels were incubated in SYBR Gold solution for 30 min, rinsed with ultrapure water, and then photographed by a CCD camera.

Nuclear magnetic resonance (NMR) spectra were recorded on a Bruker Avance 600 spectrometer equipped with a 5-mm BBI probe capable of delivering z-field gradient strength up to 50 G cm<sup>-1</sup>. Samples were prepared in Tris-HCl buffer (10 mM Tris-HCl, 90% H<sub>2</sub>O/10% D<sub>2</sub>O, pH 7.2). A standard Bruker pulse program p3919gp that applies 3–9–19 pulses with gradients was used for water suppression. 256 scans were used to acquire each spectrum with a relaxation delay of 2 s.

Circular dichroism (CD) spectra were collected from 200 to 350 nm on a Jasco-815 automatic recording spectropolarimeter with a 1-cm path-length quartz cell at 25 °C. Spectra were collected with a scan speed of 500 nm/min. Each spectrum was the average of three scans. A solution containing no oligonucleotide was used as reference, and a buffer blank correction was made for all spectra. The temperature of the cell holder was regulated by a JASCO PTC-423S temperature controller. The cuvette-holding chamber was flushed with a constant stream of dry N<sub>2</sub> gas to avoid water condensation on the cuvette exterior.

Fluorescence spectra were recorded on a Hitachi F4500 spectrofluorometer (Japan) in a 1-cm path-length quartz cell at room temperature. Xenon arc lamp was used as the excitation light source. The excitation and emission slits were both 10 nm. Excitation was set at 340 nm, and emission was collected from 350 to 650 nm. The scan speed was 240 nm/min.

### 2.3. Plasmid construction, *in vitro* transcription, and luciferase assay

To construct the plasmids, the DNA sequence of P1 promoter (LB124: –3934 to –1287) and its mutated sequences flanked with restriction sites for the enzymes KpnI FastDigest, AvrII FastDigest, and HindIII FastDigest (MBI) were synthesized in GeneArt (Germany), which have been further validated by DNA sequencing. In order to insert the plasmid into the vector, plasmids and pGL3-Basic (Invitrogen) were respectively incubated in 37 °C water bath for 2 h to ensure that all of the DNA sequences were cut by the enzyme KpnI and HindIII. The native P1 promoter constructs were then obtained by the ligation of native plasmid and pGL3-Basic in the presence of T4 DNA ligase (NEB) at 16 °C for 1 h. The native plasmid with pGL3-Basic vector, mutated plasmid was respectively digested by the enzymes AvrII and HindIII in 37 °C water bath for 2 h, and then the mutated plasmid ligated with pGL3-Basic vector by T4 DNA ligase at 16 °C for 1 h. Competitor plasmids were obtained by transformed plasmids into DH5α (Invitrogen). Both of the plasmids have been evaluated by DNA sequencing.

The A549 cells were maintained in DMEM medium with 10% FBS (Invitrogen) at 37 °C. Transfections were carried out with 5 × 10<sup>5</sup> cells/well on 6-well tissue culture plates when cells were 90% confluent. The transfections were operated according to the manufacturer's protocol, using 25 ng of pRL-TK (Renilla luciferase reporter plasmid) and 1 μg of native and mutated plasmid vector, and then the cells were incubated for 48 h at 37 °C under 5% CO<sub>2</sub>. The Renilla luciferase activity was used to normalize luciferase activity from each sample. Firefly and Renilla luciferase activities were assayed by using the Dual-Luciferase Reporter Assay System (Promega) according to the manufacturer's protocol. Experiments were repeated at least three times.

### 2.4. RNA isolation and real time polymerase chain reaction (PCR)

Exponentially growing 3 × 10<sup>5</sup> A549 cells were seeded in six-well plate on Day 1. The cells were treated with different concentrations of spermidine (0–15 μM) on Day 2. After 24 h of PD treatment, cells

were lysed for RNA isolation. The control sample included cells, which were not given any polyamine treatment. Quantification of RNA was done using a Nanodrop (ND-1000) spectrometer. The samples were then given DNase I treatment to remove DNA contamination and RNA quality was checked by running a 1% agarose gel. cDNA was synthesized using a high capacity kit (ABI) as per manufacturer's protocol. The cDNA quality was checked by PCR. This was followed by real time PCR in iQ5 (Bio-Rad) using SYBER green master mix as per manufacturer's protocol to assess the transcript level of target gene (Bcl-2) with respect to internal reference gene GAPDH. Data analysis was done to obtain fold change by Pfaffl's method [20]. The primers used for real time PCR were: Bcl-2 primers (forward primer: TGCACCTGACGCCCTTCAC; reverse primer: AGACAGCCAGGAGAAATCAACAG); GAPDH primers (forward primer: TGGTATCGTGGAAGGACTCA; reverse primer: CCAGATGAGGCAGGGA TGAT).

### 3. Results

#### 3.1. Formation of the p32 G-quadruplex

Nucleic acids show a 50–80% increase in absorbance at 295 nm upon quadruplex formation. A melting transition can be found when measuring the absorbance at 295 nm because the enhancement in absorbance is recovered upon denaturation by heating. The simple thermal melting experiment is thus feasible to evaluate the formation of quadruplex. The p32 oligonucleotide without  $K^+$  present shows no melting transition of the absorbance at 295 nm, implying that p32 exists in a random state (Fig. S1). However, a single melting transition at 295 nm with a  $T_{1/2}$  value of 82 °C can be observed when p32 is measured under the physiological  $K^+$  condition (Fig. 2a), indicating the formation of the G-quadruplex structure with a high thermal stability [21]. Adding  $Li^+$ , a cation that can destabilize G-quadruplex structure, the melting transition temperature was decreased (Fig. S2), further supporting formation of the G-quadruplex structure. Furthermore, the melting transition

temperature is concentration-independent, implying that the G-quadruplex is an intramolecularly folded structure [22].

The intramolecular structure of p32 G-quadruplex is also supported by the band-shift assay in native PAGE. It was reported that the mobility of a linear DNA in gel was slower than that of an intramolecular G-quadruplex, and faster than that of corresponding intermolecular structures [23]. According to this principle, the mutant sequence p32-mut, complementary sequence p32-com, and duplex of p32–p32com are used as a negative control. The mutant and complementary sequences cannot form a folded structure under the experimental condition and thus they keep a linear structure, while the duplex of p32–p32com represents an intermolecular structure. In a  $1 \times$  TBE gel with 100 mM KCl, p32 had the fastest mobility (Fig. S3), supporting the intramolecular G-quadruplex structure.

To further analyze the structure of p32 G-quadruplex, CD spectroscopy is used. G-quadruplexes are known to have different topologies which are classified to three types according to the sequence of glycosidic bond angles adopted by guanines [24,25]. Each type of G-quadruplex topology has its specific CD feature: parallel-type G-quadruplexes have a positive maximum at 264 nm and a negative minimum at 240 nm; antiparallel-type G-quadruplexes show a CD pattern characterized by a positive ellipticity maximum at 290 nm and a negative minimum at 264 nm; whereas hybrid-type G-quadruplexes have a negative minimum at 240 nm and two positive ellipticities at 264 nm and 290 nm respectively [24,26]. The CD spectrum of p32 showed a negative band at 238 nm and a maximum positive signal at 260 nm with a shoulder at 290 nm under the salt-deficient conditions (Fig. 2b). Though the spectrum is in accord with the CD feature of the hybrid-type G-quadruplex, p32 still exists in random DNA structure because it had no UV-melting transition temperature (Fig. S1) and the guanine imino proton signal in  $^1H$  NMR spectra (Fig. 2c). With  $K^+$  being added in, the band at 260 nm red shifted to 264 nm while the shoulder at 290 nm became a major positive band. According to the CD characteristic [24,26,27], the G-quadruplex topology of p32 may be the hybrid-type with both parallel/antiparallel features. However,

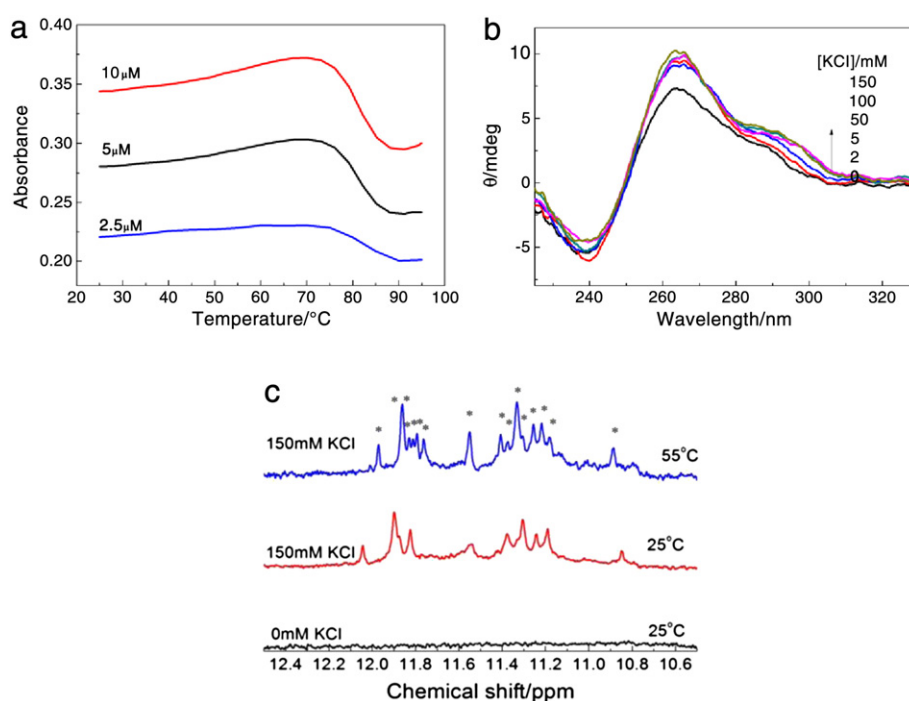


**Fig. 2.** The spectral feature of the p32 G-quadruplex. (a) Melting UV profiles of 2.5  $\mu$ M, 5  $\mu$ M, and 10  $\mu$ M p32 in 10 mM Tris–HCl buffer solution (pH 7.2) with 150 mM KCl. (b) The CD spectra of 2  $\mu$ M p32 in 10 mM Tris–HCl buffer solution (pH 7.2) without and with 150 mM KCl. (c) The part temperature-dependent  $^1H$  NMR spectra of 0.07 mM p32 with 150 mM KCl absent and present in 10 mM Tris–HCl buffer (pH 7.2, 10%  $D_2O$ ). The symbol \* corresponds to an imino proton signal.

it is also possible that p32 formed a mixture with more than two G-quadruplex topologies.

To address this issue, the  $^1\text{H}$  NMR spectra of p32 are further measured. Corresponding to G-quadruplex formation, the  $^1\text{H}$  NMR spectra show characteristic guanine imino protons with their chemical shifts within the range of 10–12 ppm [28]. If p32 forms a single G-quadruplex species, the guanine imino protons should exhibit well-resolved signals [29]. Oppositely, the guanine imino protons will exhibit broad signals. In the  $^1\text{H}$  NMR spectra of p32, several well-resolved signals appeared in the range of 10–12.5 ppm under the physiological  $\text{K}^+$  condition (Fig. 2c), meaning p32 formed a single G-quadruplex species [29]. Combined with the CD results, we can speculate that p32 G-quadruplex is a hybrid-type topology with both the parallel/antiparallel features. Rising temperature, the larger peaks split into several minor peaks, and all these peaks have been assigned to 16 imino protons (Fig. S4), implying that 16 guanines are involved in inter-guanine hydrogen bonding. The result suggests that the p32 G-quadruplex composed of four G-tetrads due to each G-tetrad contains 4 guanines.

### 3.2. Regulation of the p32 G-quadruplex conformation

As a special structure located in Bcl-2 P1 promoter, p32 G-quadruplex is expected to a target modulating Bcl-2 gene expression, and thus the ligand targeting at the G-quadruplex structure may be developed to an anticancer drug. Numerous G-quadruplex ligands have been reported to date, and most of them were evaluated by their property in inducing G-quadruplex formation or improving G-quadruplex stability [30,31]. However, the p32 G-quadruplex itself has a high thermal stability even though no ligand is present, so a further improved stability by ligands may be not so significant. There are researches that indicate that the physiological function of G-quadruplexes are conformationally relevant [32,33], which encourages us to make attempts to control Bcl-2 expression by regulating p32 G-quadruplex conformation.

A phenanthroline bisquinolinium derivative (named 2a) with two cationic side-arms, has been reported to exhibit a good selectivity to G-quadruplex and also a very high level of quadruplex stabilization [34]. The reason for 2a's excellent property is the perfect match of

the 2a molecular frame with G-quartet and electrostatic properties provided by two quinolinium side arms. Compared with 2a, PD has four substitute groups respectively locating at 2, 4, 7, 9 sites of the phenanthroline but has no cationic side-arms. The four substituents without cation charges make PD show a high selectivity to G-quadruplex versus duplex but a non-stabilizing effect on G-quadruplex (Fig. 3, Fig. S5). Furthermore, PD is also unable to induce G-quadruplex formation (Fig. S6). However, PD can induce a conformational change of the p32 G-quadruplex. These properties of PD facilitate the determination of the relevance between the G-quadruplex conformation and physiological function with no need to consider the interference of an improved G-quadruplex stability.

The conformational change of the p32 G-quadruplex induced by PD was determined by using CD spectroscopy. The p32 G-quadruplex has more parallel character with less antiparallel character according to the intensity and sharpness of the peaks at 263 nm and 290 nm (Fig. 3c). Titration of PD causes an obvious increase of antiparallel character. Served as a contrast, the telomeric hybrid-type G-quadruplex did not show any change in CD spectra with titration of PD (Fig. S7). The results implicate that the CD spectral change should originate from the p32 G-quadruplex conformational transition. In the NMR spectra, part imino proton peaks with PD are found similar to that without PD (Fig. S8), implying that the conformational transition happened not through the p32 G-quadruplex being completely denatured, in accordance with the moderate changes of the CD spectra.

### 3.3. Physiological relevance of the p32 G-quadruplex

Luciferase assay was used to further testify the physiological function the p32 G-quadruplex. A549 in 24-well plates were cotransfected with luciferase constructed or empty pGL vector as well as the internal control pRL-TK vector for 48 h (Fig. 4a). To examine the role of p32 G-quadruplex on Bcl-2 activity, we designed another pGL vector in which the central guanines in each G-tract of the p32 sequence have been mutated to thymine. The mutation is designed with the intention to inhibit the p32 G-quadruplex formation (Fig. S9) as the central guanines are obliged to form the critical core G-tetrad of any G-quadruplex [16]. Interestingly, the mutated vector shows a reduced

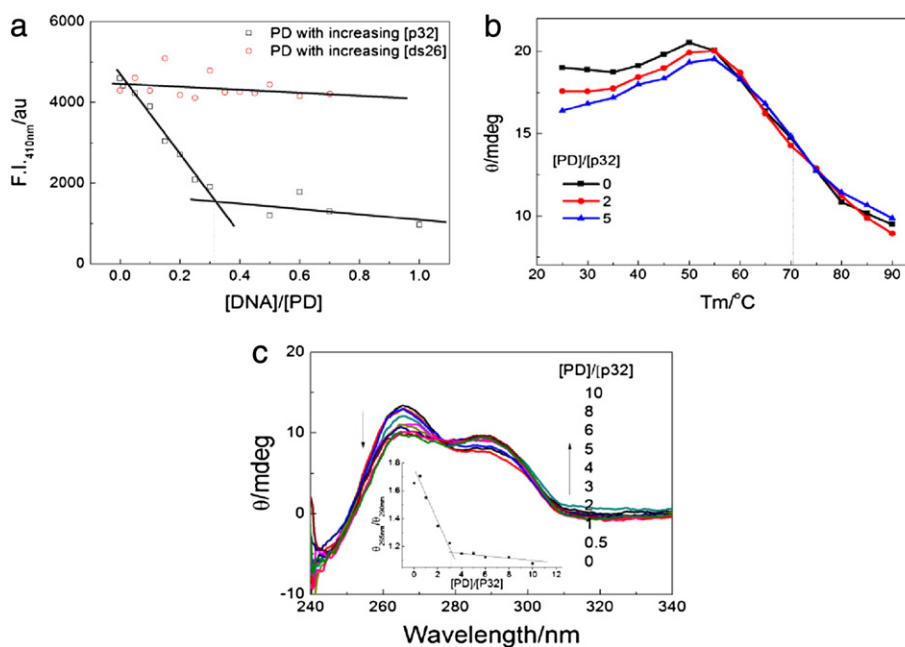


**Fig. 3.** Interaction between the p32 G-quadruplex and PD. (a) The plots of the fluorescence intensity of 3  $\mu\text{M}$  PD at 410 nm versus the ratio of  $[\text{DNA}]/[\text{PD}]$  when exciting at 330 nm. (b) The CD melting curves at 265 nm of the p32 G-quadruplexes with different concentrations in the presence of 50 mM KCl. (c) CD titration of 3  $\mu\text{M}$  p32 G-quadruplexes by increasing amount of PD in 10 mM Tris–HCl buffer solution with 150 mM KCl. The inserts are the plots of 265 nm/290 nm versus  $[\text{PD}]/[\text{DNA}]$ .

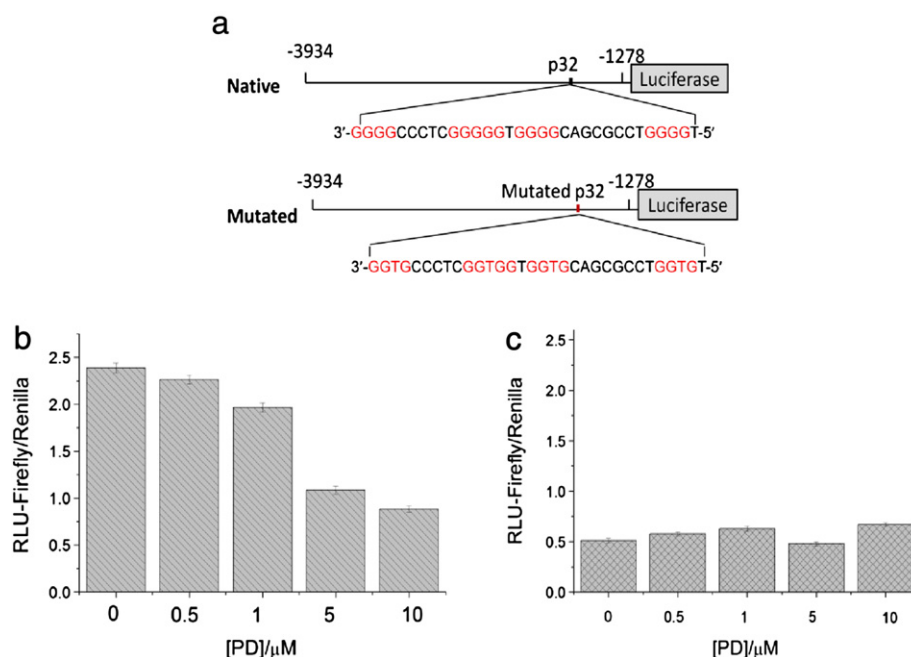


**Fig. 4.** Effect of PD on the transcription efficiency of the Bcl-2 P1 promoter. (a) Schematic representation of P1 promoter of luciferase reporter constructs: native, wild-type P1 promoter with full-length; mutated, in which the mutation from guanines to thymines has been made in the region that p32 is located. Relative transcription efficiency of (b) the native and (c) the mutated vectors in A549 cells in the absence and presence of different amounts of PD, as judged by quantitation of luciferase enzyme activity. Error bars represent the s.d. of three independent experiments.

transcription activity compared with that of the native vector (Fig. 4b, c), implicating that the p32 G-quadruplex is essential for regulating transcription.

Due to the important role of the G-quadruplex in regulating transcription, the interaction of PD with the p32 G-quadruplex is expected to affect Bcl-2 expression. A down-regulation of Bcl-2 expression in a dose-dependent manner was observed when PD was cotransfected with the native vector (Fig. 4b). Similarly, Then the real time PCR assay is operated, an inhibited Bcl-2 expression with increased amounts of PD has also been found in the real time PCR assay (Fig. S10), consisting with the luciferase result. However, a dose-independent Bcl-2 expression was found when PD was cotransfected together with the mutated vector into the cells (Fig. 4c). Since the only discrepancy for these two group assays is the absence of the p32 G-quadruplex in the mutated vector, the luciferase results demonstrate that the down-regulated Bcl-2 gene expression is caused by the interaction of PD with the p32 G-quadruplex. Furthermore, PD can only induce a conformational transition of the p32 G-quadruplexes but cannot induce G-quadruplex formation or enhance G-quadruplex stability, and thus the above results may be owing to p32 G-quadruplex conformation which is intimately related with Bcl-2 expression.

#### 4. Discussion

A large volume of evidence from genome-wide computational studies suggests prevalence of potential G-quadruplex motifs in human promoters. However, only few in vitro evidences for functional role of the G-quadruplex structure have been shown. C-myc G-quadruplex in the nuclease hypersensitive element upstream of the P1 promoter was the first case, which was shown to act as a repressor of c-myc expression [32]. Similar function was then found for the G-quadruplexes within the core promoter of human c-kit [35] and k-RAS oncogenes [36]. In these cases, G-quadruplexes play important roles in inhibiting oncogene expression. However, there is also another case in which G-quadruplex acts as an important element for the insulin-linked polymorphic region (ILPR) gene activity expression [33].

The regulatory mechanisms for G-quadruplex functional activity are supposed to be G-quadruplex-transcription factor interaction. The non-metastatic factor NM23-H2 binding to the c-myc promoter via a G-quadruplex element [37], recombinant hnRNP A1/Up1 interacting with the KRAS promoter G-quadruplex [38], myc-associated zinc-finger protein (MAZ)/poly(ADP-ribose) polymerase 1 (PARP-1) binding to the G-quadruplex element in the murine KRAS promoter [39], binding of nucleolin/hnRNP proteins to the G-quadruplex forming sequences of the VEGF promoter [40] have been demonstrated in previous studies. The ILPR G-quadruplexes promoting gene transcription are also proved that the G-quadruplex structure is necessary for the binding of some transcription factors such as Pur-1 (also known as MAZ and ZF87) and insulin-like growth factor-2 (IGF-2) [33]. Many transcription factors, including SP1, WT1, E2F, NGF, BP1, MAZ, and IGF, bind upstream of Bcl-2 P1 promoter. Most of them, such as IGF [41] and WT1 [31], can upregulate Bcl-2 transcriptional activity. Some transcription factors, such as IGF, WT1, SP1, and MAZ, also exhibit a G-quadruplex-binding tendency [42]. It is most likely for the p32 G-quadruplex structure in Bcl-2 P1 promoter to be an essential factor for some specific transcription factor binding. Under this condition, it is possible for down-modulating Bcl-2 transcription by inhibiting G-quadruplex formation or regulating G-quadruplex conformation.

To validate the above speculation, preliminary attempts are made to probe the involvement of the p32 G-quadruplex in transcription factor binding. Insulin-like growth factor-1 (IGF-1) has been first analyzed because its structure is similar to insulin and IGF-2 which exhibit high affinity binding in vitro to ILPR G-quadruplexes [43–45]. By measuring the thermal denaturing temperature of the p32 G-quadruplexes, improved thermal denaturing temperature of the p32 G-quadruplexes has been found (data not shown), implying the possible binding between the p32 G-quadruplexes and IGF-1. Encouraged by this finding, further studies about their interaction are in progress.

In summary, a new hybrid-type G-quadruplex with a high thermal stability has been identified in Bcl-2 P1 promoter. The G-quadruplex has an important physiological function in regulating Bcl-2 expression. The G-quadruplex being inhibited through base mutations and interacting with a phenanthroline derivative has caused obvious

down-regulation of Bcl-2 expression. The research provides a direct evidence of the G-quadruplex structure in Bcl-2 P1 promoter modulating transcription, implicating the potential of the p32 G-quadruplex as a novel therapeutic target.

## Acknowledgements

We thank Prof. Chuanfeng Chen for providing the PD molecule. This research was supported under the Major National Basic Research Projects (973) (Grant No. 2013CB733701), the National Natural Science Foundation of China (Grant Nos. 31200576, 21305145, 21205121, 21303225, 81072576, and 91027033), and the Chinese Academy of Sciences (Grant No. KJCX2-EW-N06-01).

## Appendix A. Supplementary data

Supplementary data to this article can be found online at <http://dx.doi.org/10.1016/j.bbagen.2014.07.014>.

## References

- [1] S. Samuel, V.F. Tumilasci, S. Olier, T.L. Nguyen, A. Shamy, J. Bell, J. Hiscott, VSV oncolysis in combination with the Bcl-2 inhibitor obatoclax overcomes apoptosis resistance in chronic lymphocytic leukemia, *Mol. Ther.* 18 (2010) 2094–2103.
- [2] F. Esposito, M. Tornincasa, P. Chieffi, I. De Martino, G.M. Pierantoni, A. Fusco, High-mobility group A1 proteins regulate p53-mediated transcription of Bcl-2 gene, *Cancer Res.* 70 (2010) 5379–5388.
- [3] G.J. Vanasse, R.K. Winn, S. Rodov, A.W. Zieske, J.T. Li, J.C. Tupper, J.J. Tang, E.W. Raines, M.A. Peters, K.Y. Yeung, J.M. Harlan, Bcl-2 overexpression leads to increases in suppressor of cytokine signaling-3 expression in B cells and de novo follicular lymphoma, *Mol. Cancer Res.* 2 (2004) 620–631.
- [4] K. Guzinska-Ustymowicz, A. Pryczynicz, A. Kemona, J. Czyzewska, Tumor budding and its relationship to p53 and Bcl-2 expression in colorectal cancer, *Anticancer Res.* 29 (2009) 3049–3052.
- [5] V. Ifandi, M. Al-Rubeai, Regulation of cell proliferation and apoptosis in CHO-K1 cells by the coexpression of c-Myc and Bcl-2, *Biotechnol. Prog.* 21 (2005) 671–677.
- [6] L. Lo Russo, L. Lo Muzio, Combination chemotherapy for head and neck cancer: the addition of Bcl-2 inhibitors, *Curr. Opin. Investig. Drugs* 10 (2009) 1325–1333.
- [7] M. Seto, U. Jaeger, R.D. Hockett, W. Graninger, S. Bennett, P. Goldman, S.J. Korsmeyer, Alternative promoters and exons, somatic mutation and deregulation of the Bcl-2-Ig fusion gene in lymphoma, *EMBO J.* 7 (1988) 123–131.
- [8] M. Harigai, T. Miyashita, A cis-acting element in the Bcl-2 gene controls expression through translational mechanisms, *Oncogene* 12 (1996) 1369–1374.
- [9] R.L. Young, S.J. Korsmeyer, A negative regulatory element in the Bcl-2 5'-untranslated region inhibits expression from an upstream promoter, *Mol. Cell. Biol.* 13 (1993) 3686–3697.
- [10] J. Dai, D. Chen, R.A. Jones, L.H. Hurley, D. Yang, NMR solution structure of the major G-quadruplex structure formed in the human Bcl2 promoter region, *Nucleic Acids Res.* 34 (2006) 5133–5144.
- [11] Y. Tsujimoto, C.M. Croce, Analysis of the structure transcripts and protein products of Bcl-2 the gene involved in human follicular lymphoma, *Proc. Natl. Acad. Sci. U. S. A.* 83 (1986) 5214–5218.
- [12] D. Sen, W. Gilbert, A sodium-potassium switch in the formation of four-stranded G4-DNA, *Nature* 344 (1990) 410–414.
- [13] P.H. Wanrooij, J.P. Uhler, T. Simonsson, M. Falkenberg, C.M. Gustafsson, G-quadruplex structures in RNA stimulate mitochondrial transcription termination and primer formation, *Proc. Natl. Acad. Sci. U. S. A.* 107 (2010) 16072–16077.
- [14] T.S. Dexheimer, D. Sun, L.H. Hurley, Deconvoluting the structural and drug-recognition complexity of the G-quadruplex-forming region upstream of the Bcl-2 P1 promoter, *J. Am. Chem. Soc.* 128 (2006) 5404–5415.
- [15] J.X. Dai, T.S. Dexheimer, D. Chen, M. Carver, A. Ambrus, R.A. Jones, D.Z. Yang, An intramolecular G-quadruplex structure with mixed parallel/antiparallel G-strands formed in the human Bcl-2 promoter region in solution, *J. Am. Chem. Soc.* 128 (2006) 1096–1098.
- [16] M.I. Onyshchenko, T.I. Gaynutdinov, E.A. Englund, D.H. Appella, R.D. Neumann, I.G. Panyutin, Stabilization of G-quadruplex in the Bcl2 promoter region in double-stranded DNA by invading short PNAs, *Nucleic Acids Res.* 37 (2011) 7570–7580.
- [17] M.I. Onyshchenko, T.I. Gaynutdinov, E.A. Englund, D.H. Appella, R.D. Neumann, I.G. Panyutin, Quadruplex formation is necessary for stable PNA invasion into duplex DNA of Bcl2 promoter region, *Nucleic Acids Res.* 39 (2011) 7114–7123.
- [18] M.W. Mayo, C.Y. Wang, S.S. Drouin, L.V. Madrid, A.F. Marshall, J.C. Reed, B.E. Weissman, A.S. Baldwin, WT1 modulates apoptosis by transcriptionally upregulating the Bcl-2 proto-oncogene, *EMBO J.* 18 (1999) 3990–4003.
- [19] S. Balasubramanian, L.H. Hurley, S. Neidle, Targeting G quadruplexes in gene promoters: a novel anticancer strategy, *Nat. Rev. Drug Discov.* 10 (2011) 261–275.
- [20] Z.Q. Hu, H.Y. Hu, C.F. Chen, Phenanthroline dicarboxamide-based helical foldamers: stable helical structures in methanol, *J. Org. Chem.* 71 (2006) 1131–1138.
- [21] P.A. Rachwal, K.R. Fox, Quadruplex melting, *Methods* 43 (2007) 291–301.
- [22] N. Kumar, S. Maiti, A thermodynamic overview of naturally occurring intramolecular DNA quadruplexes, *Nucleic Acids Res.* 36 (2008) 5610–5622.
- [23] Y. He, R.D. Neumann, I.G. Panyutin, Intramolecular quadruplex conformation of human telomeric DNA assessed with  $^{125}\text{I}$ -radioprobe, *Nucleic Acids Res.* 32 (2004) 5359–5367.
- [24] A.I. Karsisiotis, N.M. Hessari, E. Novellino, G.P. Spada, A. Randazzo, M.W. Silva, Topological characterization of nucleic acid G-quadruplexes by UV absorption and circular dichroism, *Angew. Chem. Int. Ed.* 50 (2011) 10645–10648.
- [25] S. Masiero, R. Trotta, S. Pieraccini, S.D. Tito, R. Perone, A. Randazzo, G.P. Spada, *Org. Biomol. Chem.* 8 (2010) 2683–2692.
- [26] D. Miyoshi, A. Nakao, N. Sugimoto, Structural transition from antiparallel to parallel G-quadruplex of d(G(4)T(4)G(4)) induced by  $\text{Ca}^{2+}$ , *Nucleic Acids Res.* 31 (2003) 1156–1163.
- [27] A. Ambrus, D. Chen, J.X. Dai, T. Bialis, R.A. Jones, D.Z. Yang, Human telomeric sequence forms a hybrid-type intramolecular G-quadruplex structure with mixed parallel/antiparallel strands in potassium solution, *Nucleic Acids Res.* 34 (2006) 2723–2735.
- [28] J. Feigon, K.M. Koshlap, F.W. Smith,  $^1\text{H}$  NMR spectroscopy of DNA triplexes and quadruplexes, *Methods Enzymol.* 261 (1995) 225–255.
- [29] S. Rankin, A.P. Reszka, J. Huppert, M. Zloh, G.N. Parkinson, A.K. Todd, S. Ladame, S. Balasubramanian, S. Neidle, Putative DNA quadruplex formation within the human c-kit oncogene, *J. Am. Chem. Soc.* 127 (2005) 10584–10589.
- [30] M.C. Nielsen, T. Ulven, Macrocyclic G-quadruplex ligands, *Curr. Med. Chem.* 17 (2010) 3438–3448.
- [31] Q. Li, J.F. Xiang, H. Zhang, Y.L. Tang, Searching drug-like anti-cancer compound(s) based on G-quadruplex ligands, *Curr. Pharm. Des.* 18 (2012) 1973–1983.
- [32] A. Siddiqui-Jain, C.L. Grand, D.J. Bearss, L.H. Hurley, Direct evidence for a G-quadruplex in a promoter region and its targeting with a small molecule to repress c-MYC transcription, *Proc. Natl. Acad. Sci. U. S. A.* 99 (2002) 11593–11598.
- [33] A. Lew, W.J. Rutter, G.C. Kennedy, Unusual DNA structure of the diabetes susceptibility locus IDDM2 and its effect on transcription by the insulin promoter factor Pur-1/MAZ, *Proc. Natl. Acad. Sci. U. S. A.* 97 (2000) 12508–12512.
- [34] A. De Cian, E. DeLemos, J.L. Mergny, M.P. Teulade-Fichou, D. Monchaud, Highly efficient G-quadruplex recognition by bisquinolinium compounds, *J. Am. Chem. Soc.* 129 (2007) 1856–1857.
- [35] M. Bejugam, S. Sewitz, P.S. Shirude, R. Rodriguez, R. Shahid, S. Balasubramanian, Trisubstituted isalloxazines as a new class of G-quadruplex binding ligands: small molecule regulation of c-kit oncogene expression, *J. Am. Chem. Soc.* 129 (2007) 12926–12927.
- [36] S. Cogoi, L.E. Xodo, G-quadruplex formation within the promoter of the KRAS proto-oncogene and its effect on transcription, *Nucleic Acids Res.* 34 (2006) 2536–2549.
- [37] R.K. Thakur, P. Kumar, K. Halder, A. Verma, A. Kar, J.L. Parent, R. Basundra, A. Kumar, S. Chowdhury, Metastases suppressor NM23-H2 interaction with G-quadruplex DNA within c-MYC promoter nuclease hypersensitive element induces c-MYC expression, *Nucleic Acids Res.* 37 (2009) 172–183.
- [38] M. Paramasivam, A. Membrino, S. Cogoi, H. Fukuda, H. Nakagama, L.E. Xodo, Protein hnRNP A1 and its derivative Up1 unfold quadruplex DNA in the human KRAS promoter: implications for transcription, *Nucleic Acids Res.* 37 (2009) 2841–2853.
- [39] S. Cogoi, M. Paramasivam, A. Membrino, K.K. Yokoyama, L.E. Xodo, The KRAS promoter responds to Myc-associated zinc finger and poly(ADP-ribose) polymerase 1 proteins, which recognize a critical quadruplex-forming GA-element, *J. Biol. Chem.* 285 (2010) 22003–22016.
- [40] D.K. Uribe, K. Guo, Y.J. Shin, D. Sun, Heterogeneous nuclear ribonucleoprotein K and nucleolin as transcriptional activators of the vascular endothelial growth factor promoter through interaction with secondary DNA structures, *Biochemistry* 50 (2011) 3796–3806.
- [41] S. Pugazhenthil, E. Miller, C. Sable, P. Youngi, K.A. Heidenreich, L.M. Boxer, J.E.B. Reusch, Insulin-like growth factor-I induces Bcl-2 promoter through the transcription factor cAMP-response element-binding protein, *J. Biol. Chem.* 274 (1999) 27529–27535.
- [42] P. Kumar, V.K. Yadav, A. Baral, P. Kumar, D. Saha, S. Chowdhury, Zinc-finger transcription factors are associated with guanine quadruplex motifs in human, chimpanzee, mouse and rat promoters genome-wide, *Nucleic Acids Res.* 39 (2011) 8005–8016.
- [43] J. Xiao, L.B. McGown, Mass spectrometric determination of ILPR G-quadruplex binding sites in insulin and IGF-2, *J. Am. Soc. Mass Spectrom.* 20 (2009) 1974–1982.
- [44] M. Jansen, F.M.A. van Schaik, A.T. Ricker, B. Bullock, D.E. Woods, K.H. Gabbay, A.L. Nussbaum, J.S. Sussenbach, J.L. Van den Brande, Sequence of cDNA-encoding human insulin-like growth factor-I precursor, *Nature* 306 (1983) 609–611.
- [45] A.C. Connor, K.A. Frederick, E.J. Morgan, L.B. McGown, Insulin capture by an insulin-like polymorphic region G-quadruplex DNA oligonucleotide, *J. Am. Chem. Soc.* 128 (2006) 4986–4991.